CORAL REEF HABITAT MAPPING IN THE RED SEA (HURGHADA, EGYPT) BASED ON REMOTE SENSING

Tony Vanderstraete[1,2], Rudi Goossens[2] and Tharwat K. Ghabour[3]

1. Research Assistant of the Fund for Scientific Research - Flanders (FWO-Vlaanderen); tony.vanderstraete(at)UGent.be
2. Ghent University, Department of Geography, Ghent, Belgium; rudi.goossens(at)UGent.be
3. National Research Centre, Soils and Water Use Department, Cairo, Egypt

ABSTRACT

Remote sensing can give information about the configuration and composition of coral reefs, about the biophysical parameters of the seas and oceans in which they occur and about the changes over time of these elements. This paper deals with the classification of a Landsat7 ETM+ data set in order to identify the different bottom types (macro-algae, coral, sea grass and sand) occurring on the reefs offshore Hurghada, Egypt. Before classification, the radiance values received at sensor are corrected for atmospheric and water column effects. 'Depth-invariant bottom indices' are calculated and form the basis for classification. Besides the bottom type as an ecological classification, also a geomorphological classification is made. After contextual editing of the ecological classification, both results are combined into an open-ended hierarchical classification scheme. An in-depth accuracy assessment still needs to be undertaken but a mean accuracy between 47% and 83% is to be expected.

Keywords: coral reefs, Landsat7 ETM+, Red Sea

INTRODUCTION

Although much research has already been done on coral reefs and their degradation, there is still "a critical need for detailed monitoring and assessment of reef habitats in order to better document where and how coral reefs are threatened and to understand what measures are needed to safeguard them" (1). The ideal approach would be 'multilevel sampling' (1) where detailed, locally sampled information is extrapolated to wider areas using satellite imagery. Four categories of information can be extracted from remotely sensed data: the configuration and composition of the coral reefs, the biophysical parameters of the seas and oceans in which the coral reefs occur, and the changes of these elements over time (2).

We have already used different remote sensing techniques to derive information about the location of the coral reefs (X-, Y-coordinates) and the depth at which they occur (Z-coordinates, bathymetry) (3). The scope of this paper is to investigate the possibilities of mapping different bottom types occurring on the reef systems in the Red Sea. On a regional scale, remote sensing contributes by monitoring the physical, chemical and/or ecological conditions of the Red Sea. Together with additional information, these remote sensing based results are combined in a 'Coral Reef GIS'.

In recent years many studies have dealt with different aspects of coral reef bottom type mapping using remote sensing (4-26,29). Although the emphasis is more and more on bottom-up classification of coral reefs using hyper-spectral imagery and *in situ* spectral measurements (10,26,29,30), the classic sensor-down approach based on multi-spectral data is believed to have its own merits. It has been shown that the descriptive resolution of the Landsat7 ETM+ imagery is suitable for coarse level mapping (6,11,13,14) of coral systems where charts are often inaccurate and out of date (6), for characterising reef geomorphology and classification on the community level (26), for resource inventory, cartographic mapping, baseline environmental monitoring, change detection, bathymetry (9) and for first time survey in order to locate areas which need to be surveyed in more detail. Even if the additional costs of hardware, software and trained employees are taken into ac-

count, the remote sensing approach is still more cost-effective compared to the very labour- and time-intensive traditional field-survey methods (59). This is especially important for developing countries, where most of the coral reefs occur.

According to Gitelson & Kondratyev (28) “90% of the contribution to the signal at TOA in the visible light depends on atmospheric and water surface properties”. Before the data sets can be used for bottom-type classification, some processing steps need to be undertaken in order to deal with the atmospheric and water column effects on the signal received by the sensor (16,23,30).

The radiance at sensor, L_i, can be expressed using the following water reflectance model (9,31,32):

$$L_i = L_{si} + (a_i \cdot R_{bi}) e^{-f k_i z} \quad (1)$$

With: L_{si} : mean deep water radiance

a_i : wavelength-dependent constant accounting for atmospheric effects and water surface reflection

R_{bi} : bottom reflectance

f: geometric factor accounting for path length trough water; here set to 2 (two-flow model)

k_i: effective attenuation coefficient of water for band i, accounting for absorption by the water, phytoplankton, suspended particulates and DOM, and for scattering due to turbidity (9,33)

z: depth

As can be seen from the model, the intensity of light decreases exponentially with increasing depth. The attenuation is also wavelength dependent and increases with longer wavelengths (9,27,33,41). As a consequence, if depth increases, the signal will be more attenuated and the separability of the different classes will decrease. The spectral radiances recorded by the sensor will therefore not only be dependent on the reflectance of the substrata but also on depth (9).

The most important effect on the signal for bottom type classification is believed to be the interaction with the water column. Full atmospheric correction is preferred but, strictly, this is not necessary for classification of a single scene with classification parameters derived from within the scene (4,34,35,36). Furthermore, a number of atmospheric correction methods assume a homogeneous composition of the atmosphere all over the image. The water column effect, on the contrary, will change with different depths even if horizontal and vertical homogeneity is assumed.

We are using the “depth-invariant bottom index”-technique (31) to perform the water column correction (6,9,17,22,27,37,38). Other methods of water column correction exist (4,39) but they often need ancillary data concerning the composition of the water column (40). For each pair of water penetrating bands such an index is calculated and combined to form a base for classification (8).

This technique is only applicable in clear -Type IA, IB and II- waters (9,37,40,41). This is generally not a problem since, as with most of the coral reef environmental conditions (27), the coral reefs of the Red Sea occur in clear nutrient-poor waters (42).

A combined geomorphological and ecological classification has been suggested to be the most appropriate for remote sensing of tropical coastal areas (6,9,38).

As only a coarse ecological classification is meaningful, four main bottom types (sand, macroalgae, coral and sea grass) are distinguished. The delineation of these bottom types is based on the results and schemes used by various authors for remote sensing classification (8,9,11,12,17,19,22,25,26,43). The actual ecological classification is based on the 3 depth-invariant bottom indices. Additionally, Mumby & Edwards (20) advise to add texture layers to improve the classification. Especially a better distinction can be made between the confusing coral

and sea grass classes. Sea grass is supposed to have a more homogeneous structure and corals more heterogeneous. This is only a relative indication and actual spatial texture statistics that are characteristic for reef-bottom types have yet to be determined (25).

The geomorphological classification is based on a visual digitalisation of the different features. A true colour composite of the Landsat7 ETM+ bands 1, 2, 3 and an IHS-optimised colour composite in which a shaded depth map has been integrated (4,37,44) are used as a base for digitalisation. The different classes are mainly derived from the geomorphological classification schemes worked out by Coyne et al. (24) for Hawaii and by Mumby & Harborne (8) for the Caribbean.

Due to spectral similarities of the different benthic classes, even after conversion to depth-invariant bottom indices, misclassifications are frequent due to the low spectral resolution of Landsat7 ETM+. But as coral reefs often exhibit a predictable geomorphological and ecological zonation with gradients of depth and wave exposure (45), contextual editing can be applied (6). Based on the geomorphological classification some decision rules can be set up in order to improve the accuracy of the coral reef ecological classification. To ensure that this does not create bias or misleading improvements to map accuracy, the decision rules must be applicable throughout a data set and not confined to the regions most familiar to the interpreter (6). Therefore, only general decision rules are applied which are confirmed by observations made by different authors all over the world (8,11,20,26,53).

A hierarchical classification scheme is applied to integrate both classifications. Each polygon in the resulting map will be assigned two labels independent of each other. This scheme is open-ended meaning that more details can be integrated if new classifications are made based on data sets with a different descriptive resolution (6,9).

METHODS

Study area

As a study area, the coral reefs near Hurghada, Egypt, (27°14'N, 33°54'E) situated in the northern part of the Red Sea, were selected (Figure 1).

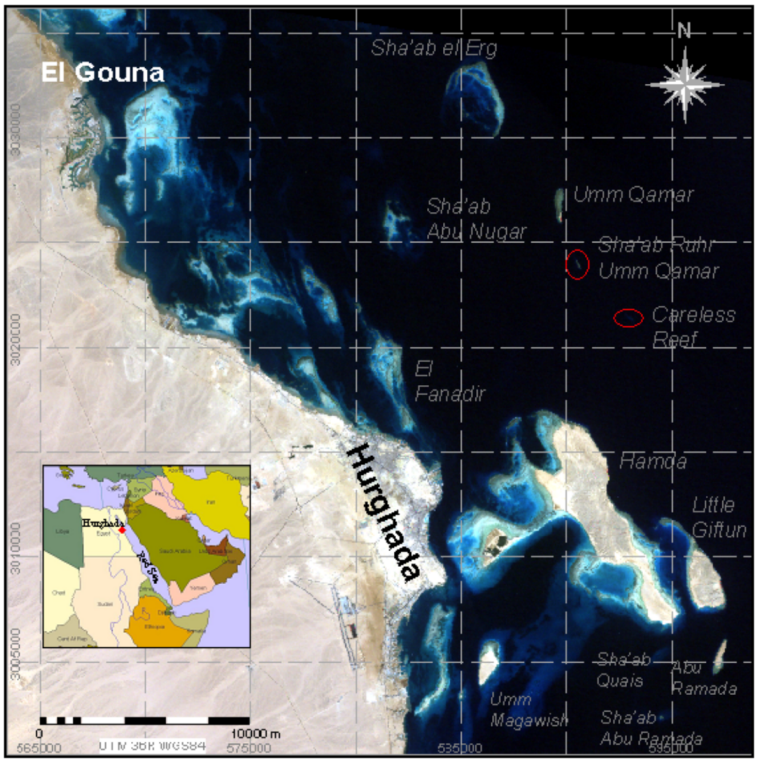

Figure 1. Localisation of the main coral reefs in the study area Hurghada (Egypt); Landsat7 ETM+ True Colour Composite (1,2,3)

The coral reefs are located in a unique environmental setting. The enclosed Red Sea is completely surrounded by deserts, has almost no water input from rivers and hence very stable physical characteristics such as salinity, temperature and water quality (42). Although the coral reefs are not under great natural threat, they are suffering from the negative effects of booming tourism and from urban coastal development projects mainly for tourist accommodation and in support of the Egyptian relocation policy.

Data

Field survey

Two field surveys have been completed between August 25th, and August 31st, 2001 and between March 28th, and April 4th, 2002. During these campaigns, 420 observations were made at sea. Emphasis was put on depth measurements and some bottom type observations were made. X- and Y-coordinates were measured using a GPS (Garmin GPS 12 XL) in the UTM36-WGS84 coordinate system.

Satellite imagery

A level-1G Landsat7 ETM+ data set (ID: LE7174041000025450; path/row: 174/041) dating from September 10th, 2000 is used to classify the main bottom types occurring in the sublittoral zone of the study area. Wavebands 1, 2 and 3 are used as the radiation within these wavelengths is not totally absorbed by the water column. The ILWIS 3.0–software is utilised to georeference a subscene covering the study area. As ground control points, 21 out of a total of 63 points measured on the land during the two field surveys, are used. The georeference is based on the specific UTM-coordinate system using a 'full second order' equation.

As most of the algorithms used in this paper are dealing with radiance values, the DN-values (byte size) as defined in the spectral bands are converted to radiance values at sensor (W/(m² sr µm)). The characteristics for this conversion can be found in the Landsat7 Science Data Users Handbook (46).

Atmospheric and water column correction

Atmospheric correction

Before the "depth-invariant bottom index"–algorithm (31) is applied to the radiance bands a rough atmospheric correction is applied based on the dark pixel subtraction method (47). Inside optically deep water most of the visual light is absorbed. As a consequence, the signal received at sensor is nearly entirely composed of atmospheric path radiance and surface reflection. If atmospheric and water surface conditions are assumed to be uniform throughout the scene, the mean deep water radiance at sensor can be used to remove the atmospheric effect and the effect of surface reflectance on the signal (9,40,48). To determine the mean deep water radiance, an area is selected in the data set where depths are known to be greater than 50m (3). As suggested by Armstrong (49), 2 standard variations are subtracted from the mean in order to account for possible sensor noise (Table 1).

Table 1: Determination of mean deep water radiance

	$L_{deep\ min}$	$L_{deep\ max}$	$L_{deep\ mean}$	St. dev.	L_{si}
Band 1	59.660	71.421	64.55	1.37	61.81
Band 2	34.573	44.219	38.57	0.98	36.61
Band 3	19.409	29.736	24.52	1.02	22.48

Water column correction

The exponential relationship between radiance and depth as expressed in equation 1, is linearised by transforming the atmospherically corrected radiance using natural logarithms (9,31,32,35,38):

$$\ln(L_i - L_{si}) = \ln(a_i \cdot R_{bi}) - 2k_i z \qquad (2)$$

If the effect of depth on measured radiance has been linearised and the substratum is constant, pixel values for each band will vary linearly according to depth (9) (Figure 2).

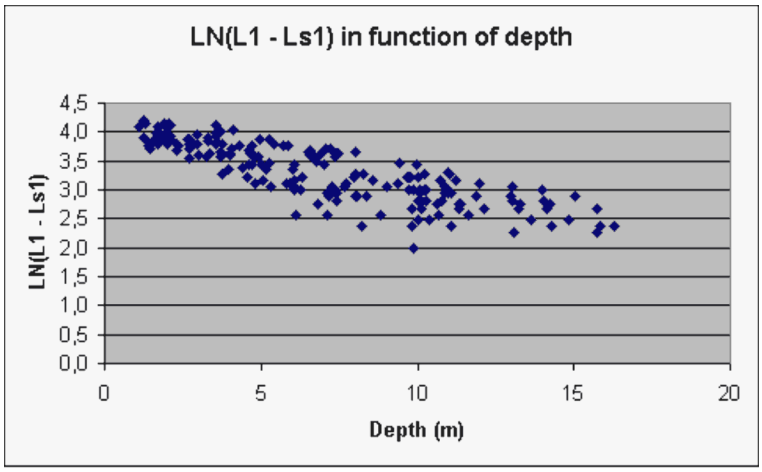

Figure 2: Log-transformed, atmospherically corrected radiance band 1 plotted against depth.

To determine the bottom reflectance, R_{bi}, equation 2 can be rearranged to:

$$\ln R_{bi} = \{\ln(L_i - L_{si}) + 2k_i z\}/a_i \quad (3)$$

However, 3 variables (a_i, k_i, z) remain unknown. The method of Lyzenga (31) does not estimate k_i for each band but uses a ratio of attenuation coefficients between a pair of bands. This ratio can be determined from the data itself and cancels out the need to know a_i and z (9).

In order to define these ratios k_i/k_j between pairs of bands a selection of pixels over uniform substratum but with variable depth is needed (9,38). A sandy bottom type is preferable (9) as it is fairly easily recognisable by the interpreter. Edwards (38) selects areas of homogeneous sandy substrate, but Maritorena (27) prefers to determine the ratio as the mean of ratios defined between pairs of pixels. We have selected a number of pixels that correspond to the field measurements made. In that way, we ensure a total coverage of depth over a fairly homogeneous sandy substrate.

Another criterion in selecting pixels is that saturation or total absorption in one of the bands should be avoided (38). This means that pixels over very shallow (<1 m) or very deep areas are discarded. Optically deep water is determined by the maximum depth of penetration of each band as calculated by Vanderstraete et al. (3).

Table 2: Maximum depth of penetration for each radiance band

	Maximum depth of penetration (m)
Band 1	21.4
Band 2	16.8
Band 3	5.2

As a result, 196 points between 1 and 16.8 m are selected for the determination of ratio k_1/k_2 ;and 79 points between a depth of 1 and 5.2 m for the determination of ratios k_1/k_3 and k_2/k_3 .

The selected pixel radiances can be represented on a bi-plot of 2 log-transformed radiance bands *i* and *j* (Figure 3). As the relationship between radiance and depth has been linearized and the substratum is constant, the pixels will fall ideally on a straight line. The slope of this 'straight line' represents the relative amounts of attenuation in each band and thus the requested ratio k_i/k_j (38). In reality, however, the points are not falling on a perfect line due to natural heterogeneity of the different bottom types, variations in water quality, surface roughness, etc. (38) (Figure 3).

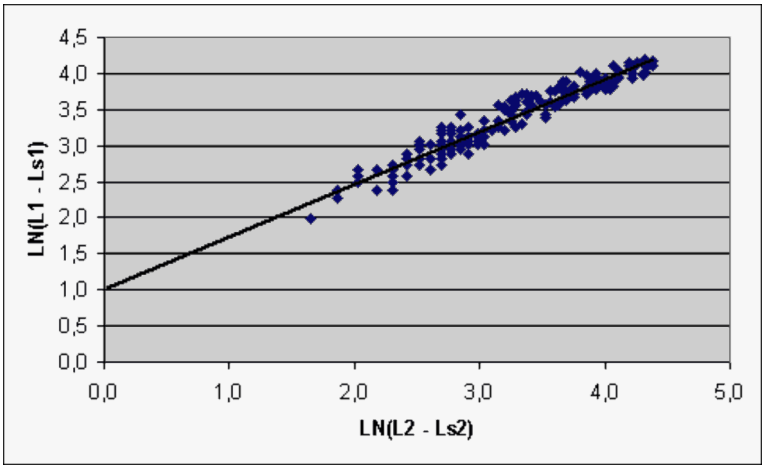

Figure 3: Bi-plot of 2 log-transformed, atmospherically corrected radiance bands

To determine the 'straight line' the least squares regression is not used as the result will depend on which band is used as the dependent variable (38). Instead, rather than calculating the mean square deviation from the regression line in the direction of the dependent variable, the regression line is placed where the mean square deviation is minimised (38):

$$k_i / k_j = a + \sqrt{a^2 + 1} \tag{4}$$

$$a = (\delta_{ii} - \delta_{jj}) / \delta_{ij} \tag{5}$$

with: δ_{ii} = variance of band i

δ_{ij} = covariance of bands i and j

Table 3. Variance within each radiance band

	Band 1	Band2	Band3
Variance δ_{ii}	0.259	0.130	0.462

Table 4. Determination of ratio k_i/k_j

	Ratio 1/2	Ratio 1/3	Ratio 2/3
Covariance δ_{ij}	0.328	0.149	0.232
a_{ij}	-0.293	-1.331	-1.713
k_i/k_j	0.75	0.33	0.52

The different ratio-values (Table 4) are in accordance with the values summarized by Green et al. (9).

If different bottom types were represented in such a bi-plot, they would all be represented by another, similar line in which variation along the line would only indicate changes in depth (Figure 4). These lines will differ in position since each bottom type has a different reflectance. The gradient of each line would be identical since the ratio of attenuation coefficients is not dependent on bottom type (9,38). The y-intercept of each line is then used as an index of bottom type independent of depth.

As not all pixels lie along a perfectly straight line (Figure 4), each pixel is assigned to an index of bottom type by connecting it to the Y-axis along a line of gradient k_i/k_j. In this way the depth-invariant index is scaled to the y-intercept (9,38). Based on this value on the Y-axis, representing the index of bottom type, the pixels are then classified. As a consequence the classification will no longer be based on the bottom spectral characteristics. Lyzenga (31), and also Maritorena (27),

perform an additional orthogonal rotation to align the y-axis along the k_i/k_j gradient. However, such a refinement does not change the functionality of the process (9).

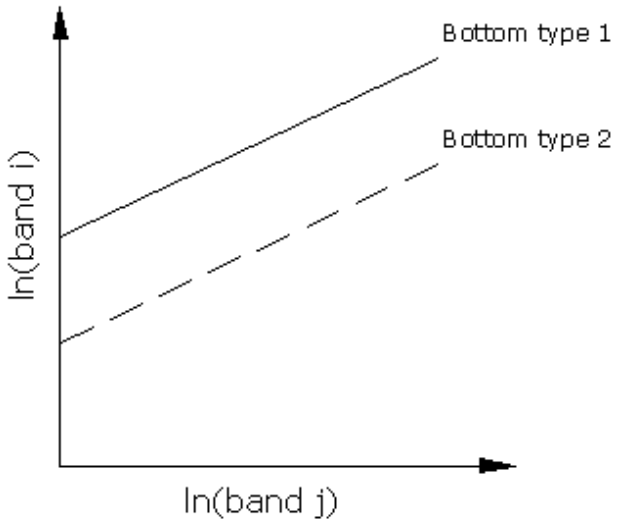

Figure 4. Difference in depth-invariant bottom index between two bottom-types

The depth-invariant bottom index (*DIB*) is defined as:

$$DIB_{ij} = X_i - \left\{ \frac{k_i}{k_j} \cdot X_j \right\} \tag{6}$$

With: band *i* along the y-axis and band *j* along the x-axis.

$X_i = \ln(L_i - L_{si})$: log-transformed atmospherically corrected radiance

k_i / k_j : ratio of attenuation coefficients

Prior to implementation it is suggested to mask out land, clouds and deep water (17,27,38). A land mask, generated from the digitised coastline (3), is applied and all land pixels are set to a value of zero. In our findings, however, the results are not improved by masking out the deep water areas before implementation. Therefore the deep water mask will only be applied to the final resulting classification.

Some values of depth-invariant bottom indices are negative, so an offset is incorporated to make all data positive (9). Furthermore, ILWIS 3.0 requires byte-maps to perform a supervised classification, hence the index-values are rescaled to the range [0,255].

Classification

Ecological classification

Because of the relatively coarse descriptive resolution of Landsat7 ETM+ imagery, only a coarse level classification can be achieved. The five main classes that are distinguished are summarized in Table 5.

Although the classification is no longer based on spectral characteristics but on depth-invariant bottom indices, a differentiation between intertidal and subtidal sand has been made because of the important spectral differences between submerged and exposed sandy substrate.

A supervised, maximum likelihood classification is effected on a map list containing 3 land-masked depth-invariant bottom indices and 3 texture layers calculated for each DIB. The texture of the objects is defined by the variance within the data (20). A 3*3 (20) variance filter is applied on the three depth-invariant bottom indices. In contrast to the depth-invariant bottom indices calculated

earlier, the DIB's used here, are calculated without applying a land mask. The added mask creates artificially high variance along the coastline. This would have a negative effect on the classification. The texture maps are then converted to image-domain [0,255] using a histogram equalisation.

Table 5. Main ecological bottom-type classes

Level 1	Level 2
Bare substrate:	sand intertidal
	sand subtidal
Benthic community:	macro-algae dominated
	coral dominated
	sea grass dominated
Land	
Deep water	
No data	

Geomorphological classification

An adaptation of the geomorphological classification schemes worked out by Coyne et al. (24) for Hawaii and by Mumby & Harborne (8) for the Caribbean is given in Table 6.

Table 6. Main geomorphological classes

Class	Description
1. land	as defined by the land mask
2. lagoon	shallow area (relative to the deeper water of the bank/shelf) protected from high-energy waves by a reef crest
3. patch reef	relatively small coral formations with unclear morphology formed by hard corals or dead coral colonised by new organisms
3.1 dense patch reef	areas of aggregated coral colonies where colonies cover more than 70% of the benthos (8)
3.2 diffuse patch reef	areas of dispersed coral colonies where less than 30% of the benthos is covered by coral colonies (8)
4. back reef	shallow zone at the landward edge of a reef crest often formed by a pavement of hard substratum with or without rubble and frequently covered with algae.
4.1 reef flat (24)	back reef between the landward edge of the reef crest and the shore
5. reef crest	the shallowest and often emergent part of a reef; it separates fore reef from back reef and lagoon.
6. fore reef	zone seaward of reef crest (often difficult to distinguish from bank/shelf)
6.1 spur and groove	spurs are usually formed by accreting hard coral and calcified green algae whereas grooves usually contain sand or bare bedrock (9)
8. bank/shelf	zone with depths to 20-30m without clear reef characteristics
9. deep water	zone with depths greater than 30m where no significant spectral reflectance is recorded by the Landsat7 ETM+ sensor
10. unknown	class containing areas of undefined nature

A true colour composite and a 'depth-improved' colour composite are then used to visually digitise the different geomorphological features. In order to create the shaded depth map used in the 'depth-improved' colour composite, a shadow filter has been applied on a bathymetric map of the area (3). Best results are returned when a filter initialising the sun in the northeast is applied. This direction is in line with the dominant surface currents in the area (42). The shaded depth map is

then fused with ETM+ band 1 and 2 using a classic IHS data fusion technique (50-52) in which the intensity band is replaced by the shadow map (4,37).

The different geomorphological features are then delineated based on their spectral and geomorphologic, i.e. bathymetric, characteristics.

Post-classification: contextual editing

Three decision rules are applied in order to improve the ecological classification:

- If the ecological class “sea grass dominated” occurs on the geomorphological class “fore reef”, it is replaced by the ecological class “coral dominated” (8,20,26).
- If the ecological class “sea grass dominated” occurs on the geomorphological class “reef crest”, it is replaced by the ecological class “coral dominated” (8,20,26,53).
- If the ecological class “sea grass dominated” occurs on the geomorphological class “back reef” and depth is lower then 1.2m, it is replaced by the ecological class “macro-algae dominated” (8,11,26).

Finally, two masks are applied to deal with misclassifications in land and deep-water areas. The land mask is the same as the one used for the calculation of the depth-invariant bottom indices. The deep water is defined during geomorphological mapping as those areas where no significant reflection of the seabed is noticed.

RESULTS

Effect of water column correction

If Figures 5 and 6 are compared, the effect of the water column correction can clearly be seen. In Figure 5 the raw radiance data are represented as a function of depth. A distinctive exponential relationship can be noticed between them, especially in the first metres. The depth-invariant bottom indices, on the contrary, are almost totally independent of depth (Figure 6).

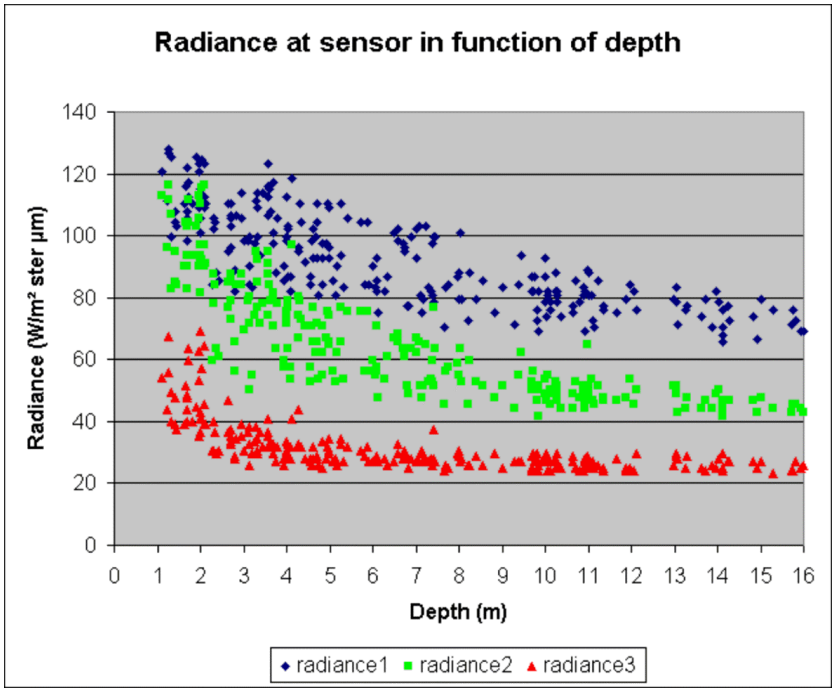

Figure 5: Radiance as a function of depth

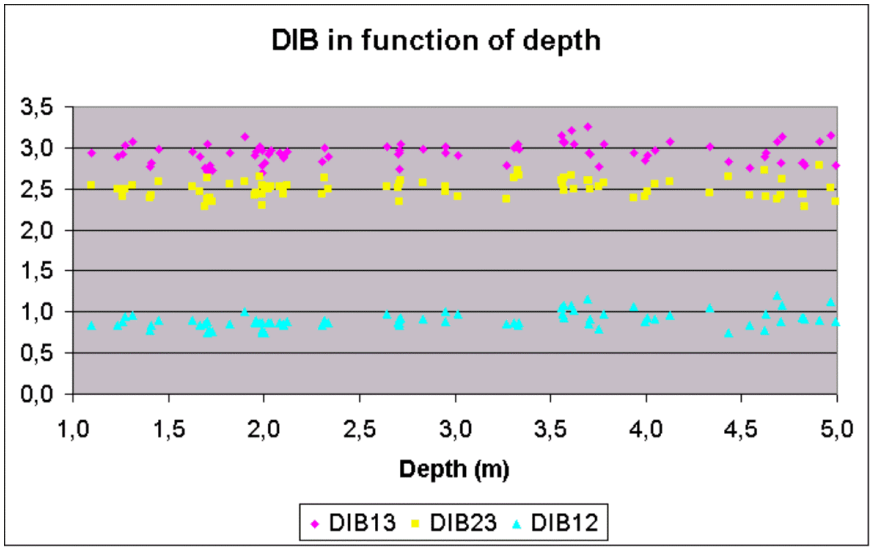

Figure 6: Depth-invariant bottom indices as a function of depth

Ecological classification

The result of the ecological classification before contextual editing is shown in Figure 7. The class "no data" is due to pixels with radiance values, L_i, smaller than mean deep-water radiance, L_{si}. These values only occur over deep water and do not affect the overall classification result.

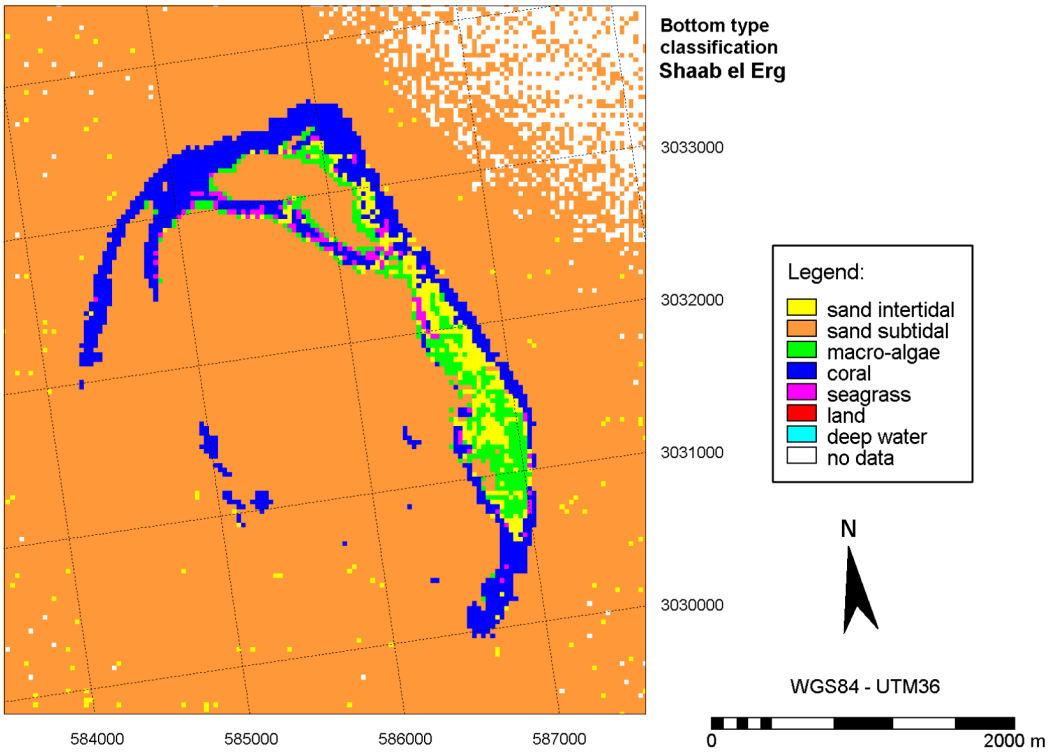

Figure 7: Bottom-type classification of the Shaab el Erg-sub area

Geomorphological classification

The result of the geomorphological classification is represented in Figure 8. The original polygon map is rasterised to 30m in order to match it with the resolution of the ecological classification.

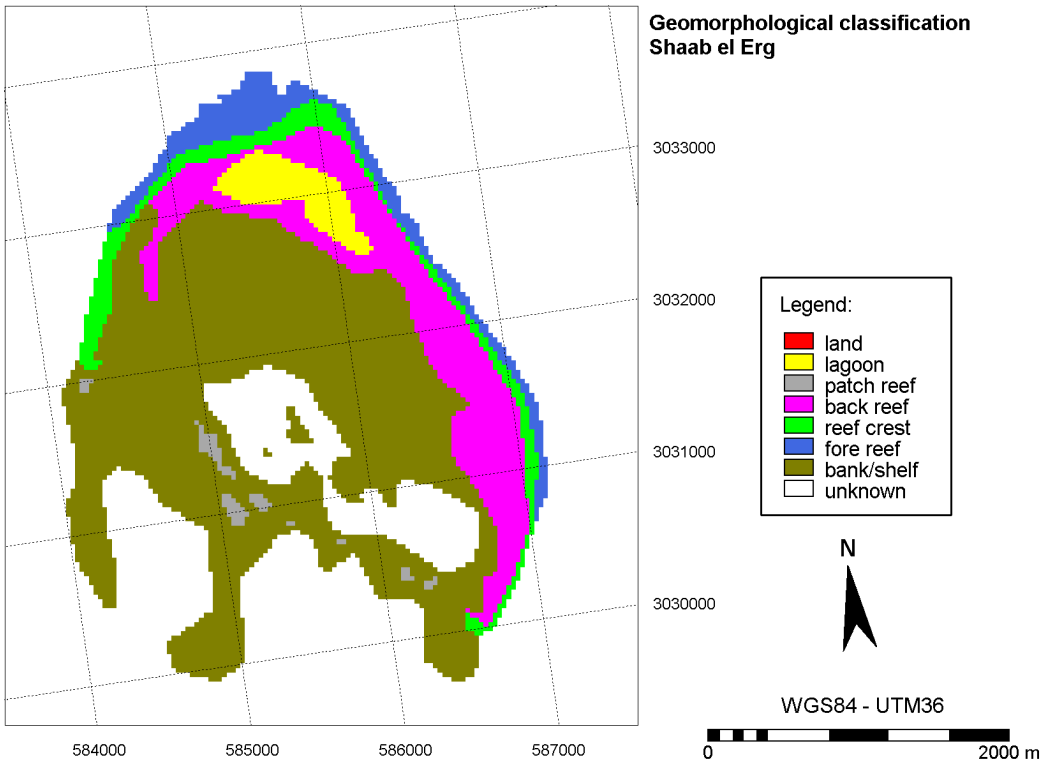

Figure 8: Rasterised geomorphological classification of Shaab El Erg

Ecological classification after contextual editing

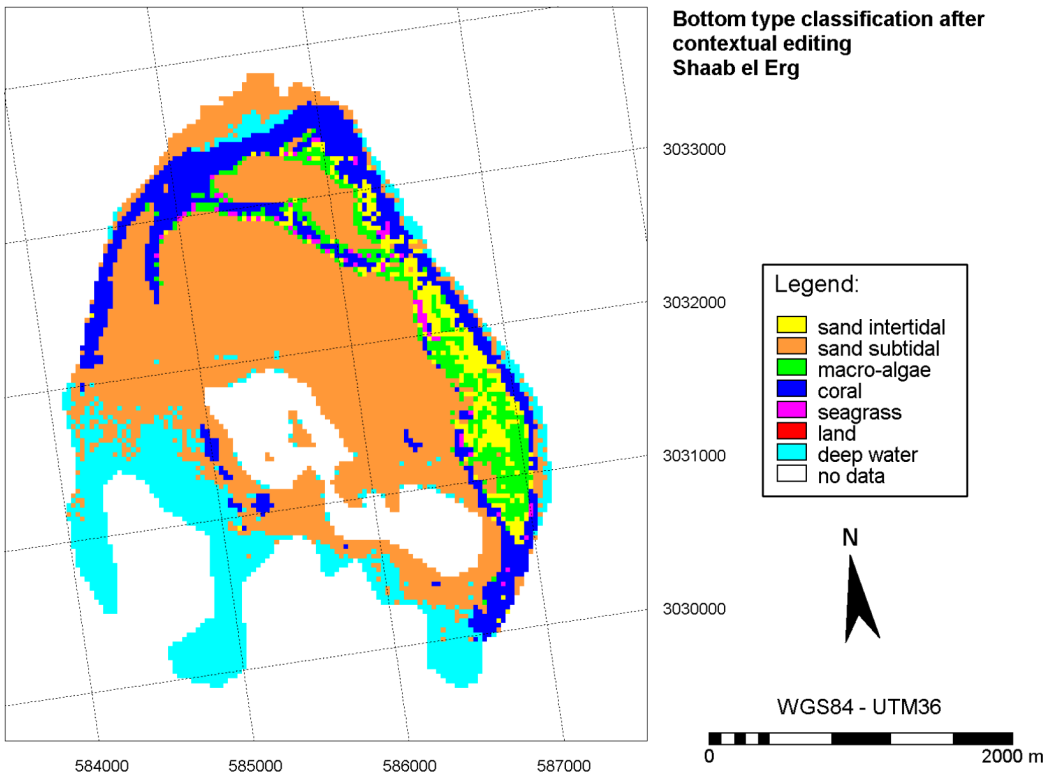

Figure 9. Bottom-type classification of the Shaab el Erg-sub area after contextual editing

After the application of the defined decision rules, the resulting ecological classification is given in Figure 9. The 'deep water' class represents areas that are recognised on the geomorphological classification but that lie lower than the maximum depth of penetration of each radiance band (3).

Hierarchical classification

As a final result the ecological and geomorphological classifications are integrated into one hierarchical classification map (Figure 10). The colours represent the geomorphological features; the patterns symbolize the associated bottom-types.

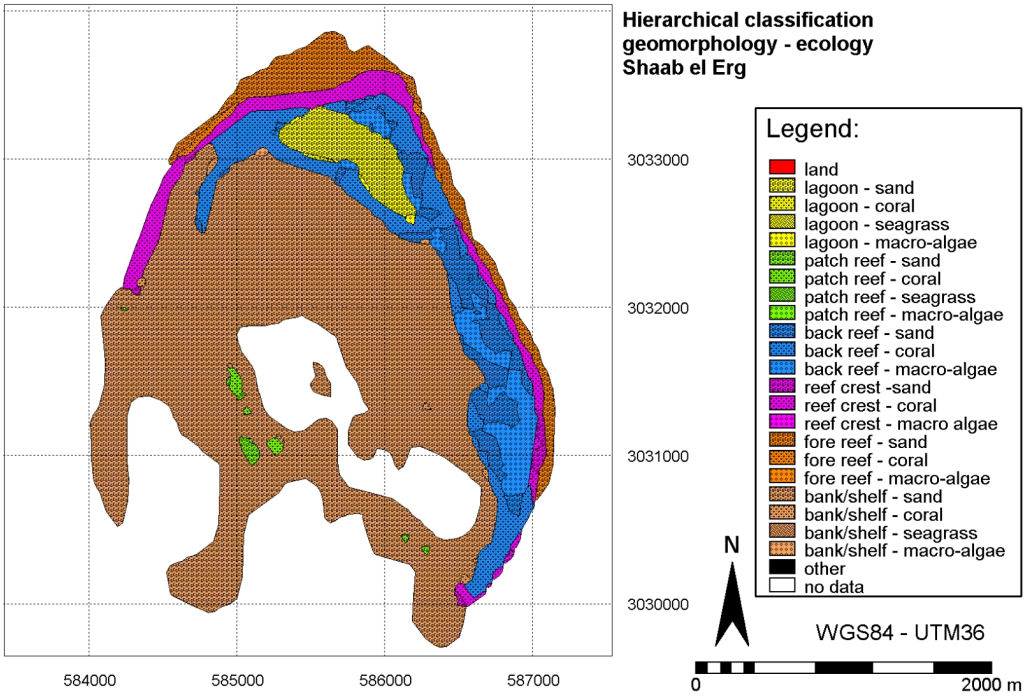

Figure 10: Hierarchical classification map of the Shaab el Erg-sub area.

DISCUSSION

Mumby (6) has pointed out the significant improvement to map accuracy for Landsat TM bottom-type classification at coarse and intermediate descriptive levels when a water column correction is applied. The effect of water column correction is clearly shown in Figure 6. This improvement is also statistically proven when the coefficients of variation are compared between the original radiance bands and the resulting depth-invariant bottom indices (9,38).

Table 7. Overview of Coefficients Of Variation (COV) based on 79 ground control points;
** based on 247 ground control points*

	COV
Radiance 1	0.160399*
Radiance 2	0.186056
Radiance 3	0.2752
DIB12	0.105776
DIB13	0.041860
DIB23	0.042636

As can be seen in Table 7, the COV of each depth-invariant bottom index is much lower than the COV of the corresponding radiance bands. This is the result of the elimination of the variation caused by the water column (9,38). Nevertheless it should be noted that the water column correction is optimised for a sandy bottom type. This will lead to an improvement for mapping sand habitats but could possibly also lessen differentiation between the other bottom-types (6).

Mumby (20) is doubtful about the positive effect of integrating texture layers into the ecological classification. Due to the use of a 3·3 variance filter the classification scale is reduced to 90*90m in the case of Landsat7 ETM+. This texture resolution is believed to reflect interclass rather then intraclass heterogeneity (20). Nevertheless, in our findings, the use of texture layers in combination with the depth-invariant bottom indices, does improve the resulting classification map.

The effect of contextual editing has already been pointed out by Mumby (6). Especially in combination with water column correction, the coarse level classification of a Landsat data set is significantly improved (6). A quantitative estimation of the effect of all these elements can only be made after an accuracy assessment has been made.

To test accuracy, we need a sufficiently large set of independent field observations (9). Previous field observations have primarily concentrated on depth measurements over homogeneous sandy substrates (3). Hence, field observations over other bottom types were limited and are insufficient for a thorough accuracy testing. A new field survey is planned in the near future to deal with this problem.

However, the classification of bottom type can never be 100% accurate. First of all, the nature itself of the bottom types is very complex (9). The boundaries of ecological habitats tend to be gradiential and not clear, distinct lines. The delineation and definition of habitats will therefore always be slightly arbitrary. Even with a bottom-up classification (26) and a full spectral resolution of 1nm over a spectral range from 400 to 700nm, Hochberg (26) reached only a maximum accuracy of 83%. He also determined a maximum mean accuracy of 47% with Landsat7 ETM+ if 12 bottom types are distinguished (26).

What are then the main problems in the classification of bottom types based on remote sensing? First of all errors are made due to the basic assumption of vertical and horizontal homogeneity of the atmosphere and water column (25,29). Besides, not only the gradient between different bottom types is important, but also the structural composition and geomorphology of the reef. The classification accuracy is limited by the slope and aspect of the benthic topography (29), the 3-D arrangement of the reef (25) and the resulting effect of light and shadow (25,54).

The bottom types of the benthic community have also a remarkable spectral similarity. As the symbiotic zooxanthellae and not the coral polyp-tissue are mainly causing the colour of living hard and soft corals (15,17,20), the spectral signature of the coral becomes similar to that of the sea grasses and macro-algae. This makes the discrimination between these bottom types even more problematic taking the low spectral resolution of the Landsat7 ETM+ into account (25).

The time lag between data acquisition and field survey also can cause some errors (11,21,55-57), although Mumby (20) shows that habitats most probably do not move more then 10 metres in a couple of years.

A multi-spectral distinction between coral, sea grass, macro-algae and sand can only be made up to the depth at which the red band is totally attenuated (19,58). Areas deeper than ± 5 m are then only classified on DIB_{12}, as this depth-invariant bottom index is not based on the attenuated red radiance band. As a consequence, from a depth of 10-15m only sand (26) or prominent reef features (19,40,58) can be distinguished and accurately classified.

CONCLUSIONS

The main constraints with the classification of reef bottom type based on a Landsat7 ETM+ data set are due to the assumptions inherent to the methods used, the descriptive resolution of the sensor and the natural, structural and spectral characteristics of the study object. Nevertheless, it is possible to make a coarse level ecological and geomorphological classification of the coral reefs offshore Hurghada, Egypt. The bottom type map has been improved by the application of a water column correction technique, by the integration of texture layers in the supervised classification and by post-classification contextual editing. The use of a true colour composite in combination with an IHS-optimised colour composite with integrated depth map, makes it possible to accurately delineate the different geomorphological features of a coral reef system. Finally, it is important to

integrate both classification results into an open-ended hierarchical classification scheme in order to update the maps with more detailed information from classification of satellite imagery with a higher descriptive resolution or from detailed field surveys and other ancillary information sources. A thorough accuracy assessment must be worked out in the near future in order to quantitatively estimate the usefulness of the maps produced.

REFERENCES

1 Bryant D, L Burke, J McManus & M. Spalding, 1998. Reefs at risk - a map-based indicator of threats to the world's coral reefs. (World Resources Institute)

2 Phinn S R, C Menges, G J E Hill & M Stanford, 2000. Optimizing Remotely Sensed Solutions for Monitoring, Modelling, and Managing Coastal Environments. Remote Sensing of Environment, 73(2): 117-132

3 Vanderstraete T, R Goossens & T K Ghabour, in press. Bathymetric mapping of coral reefs in the Red Sea (Hurghada, Egypt) using Landsat7 ETM+ data. Belgeo

4 Bierwirth P N, T J Lee & R V Burne, 1993. Shallow Sea-Floor Reflectance and Water Depth Derived by Unmixing Multispectral Imagery. Photogrammetric Engineering & Remote Sensing, 59(3): 285-324

5 Chauvaud S, C Bouchon & R Manière, 1998. Remote sensing techniques adapted to high resolution mapping of tropical coastal marine ecosystems (coral reefs, sea grass beds and mangrove). International Journal of Remote Sensing, 19(18): 3625-3639

6 Mumby P J, C D Clark, E P Green & A J Edwards, 1998. Benefits of water column correction and contextual editing for mapping coral reefs. International Journal of Remote Sensing, 19(1): 203-210

7 Mumby P J, E P Green, C D Clark & A J Edwards, 1998. Digital analysis of multispectral airborne imagery of coral reefs. Coral Reefs, 17: 59-69

8 Mumby P J & A R Harborne, 1999. Development of a systematic classification scheme of marine habitats to facilitate regional management and mapping of Caribbean coral reefs. Biological Conservation, 88(2): 155-163

9 Green E P, P J Mumby, A J Edwards & C D Clark (Ed. A.J. Edwards), 2000. Remote sensing handbook for Tropical Coastal Management. (Coastal Management Sourcebooks 3, UNESCO)

10 Holden H & E LeDrew, 2000. Accuracy Assessment of Hyperspectral Classification of Coral Reef Features. Geocarto International, 15(2): 5-11

11 Palandro D, 2000. Coral Reef Change Detection Using Landsats 5 and 7: A Case Study using Carysfort Reef in the Florida Keys. (College of Marine Sciences, University of South Florida (masters thesis))

12 Andréfouët S, F Muller-Karger, E Hochberg, C Hu & K Carder, 2001. Change detection in shallow coral reef environments using Landsat 7 ETM+ data. Remote Sensing of Environment, 78: 150-162

13 Dustan P, E Dobson & G Nelson, 2001. Landsat Thematic Mapper: Detection of Shifts in Community Composition of Coral Reefs. Conservation Biology, 15(4): 892-902

14 Joyce K E & S R Pinn, 2001. Optimal Spatial Resolution for Coral Reef Mapping. In: Proceedings of IGARSS 2001: 'Scanning the present and resolving the future' (IEEE: Sydney, Australia), 3p., CD-ROM

15 Kutser T, W Skirving, J Parslow, L Clementson, T Done, M Wakeford & I Miller, 2001. Spectral discrimination of coral reef bottom types. In: Proceedings of IGARSS 2001: 'Scanning the present and resolving the future' (IEEE: Sydney, Australia), 3p., CD-ROM

16 Lubin D, W Li, P Dustan, C H Mazel & K Stamnes, 2001. Spectral Signatures of Coral Reefs: Features from Space. Remote Sensing of Environment, 75(1): 127-137

17 Matsunaga T, A Hoyano & Y Mizukami, 2001. Monitoring of coral reefs on Ishigaki Island in Japan using multitemporal remote sensing data. International Society for Optical Engineering (SPIE), 11 p.

18 Holden H, 2002. Characterisation of optical water quality in Bunaken National Marine Park, Northern Sulawesi. Singapore Journal of Tropical Geography, 23(1): 23-36

19 Maeder J, S Narumalani, D C Rundquist, R L Perk , J Schalles, K Hutchins & J Keck, 2002. Classifying and Mapping General Coral-Reef Structure Using Ikonos Data. Photogrammetric Engineering & Remote Sensing, 68(12): 1297-1305

20 Mumby P J & A J Edwards, 2002. Mapping marine environments with IKONOS imagery: enhanced spatial resolution can deliver greater thematic accuracy. Remote Sensing of Environment, 82(2-3): 248-257

21 Purkis S, J A M Kenter, E K Oikonomou & I S Robinson, 2002. High resolution ground verification, cluster analysis and optical model of reef substrate coverage on Landsat TM imagery (Red Sea, Egypt). International Journal of Remote Sensing, 23(8): 1677-1698

22 Radiarta I N, N K Tripathi, F Borne & K R Jensen, 2002. Coral Reef Habitat Mapping: A Case Study in Mensanak Island - Senayang Lingga, Riau Province, Indonesia. GISdevelopment.net, Map Asia 2002, accessed: 12/01/2003.
http://www.gisdevelopment.net/application/nrm/coastal/mnm/

23 Tanis F J & N P Malinas, 2002. Shallow Water Extraction Algorithm for Bathymetry and Bottom Features. In: Proceedings of the Seventh International Conference on Remote Sensing for Marine and Coastal Environments (Veridian, Ann Arbor (MI: USA)), 8p., CD-ROM

24 Coyne M S, T A Battista, M Anderson, J Waddell, W Smith, P Jokiel, M S Kendall & M E Monaco, 2003. Benthic Habitats of the Main Hawaiian Islands. (NOAA Technical Memorandum NOS NCCOS CCMA 152 (On-line), NOAA). Accessed: 04/04/2003,
http://biogeo.nos.noaa.gov/projects/mapping/pacific/

25 Hochberg E J, M J Atkinson & S Andréfouët, 2003. Spectral reflectance of coral reef bottom-types worldwide and implications for coral reef remote sensing. Remote Sensing of Environment, 85(2): 159-173

26 Hochberg E J & M J Atkinson, 2003. Capabilities of remote sensors to classify coral, algae, and sand as pure and mixed spectra. Remote Sensing of Environment, 85(2): 174-189

27 Maritorena S, 1996. Remote sensing of the water attenuation in coral reefs: a case study in French Polynesia. International Journal of Remote Sensing, 17(1): 155-166

28 Gitelson A A & K Ya Kondratyev, 1991. Optical models of mesotrophic and eutrophic water bodies. International Journal of Remote Sensing, 12(3): 373-385

29 Holden H & E LeDrew, 2002. Measuring and modelling water column effects on hyperspectral reflectance in a coral reef environment. Remote Sensing of Environment, 81(2-3): 300-308

30 Holden H & E LeDrew, 2001. Effects of the Water Column on Hyperspectral Reflectance of ubmerged Coral Reef Features. Bulletin of Marine Science, 69: 685-699

31 Lyzenga D, 1978. Passive remote sensing techniques for mapping water depth and bottom features. Applied Optics, 17(3): 379-383

32 Paredes J M & R E Spero, 1983. Water depth mapping from passive remote sensing data under a generalized ratio assumption. Applied Optics, 22(8): 1134-1135

33 Gould R W Jr, R A Arnone & M Sydor, 2001. Absorption, Scattering, and Remote Sensing Reflectance Relationships in Coastal Waters: Testing a New Inversion Algorithm. Journal of Coastal Research, 17(2): 328-341

34 Singh A, 1989. Digital change detection techniques using remotely-sensed data. International Journal of Remote Sensing, 10(6): 989-1003

35 Andréfouët S, F Muller-Karger, E Hochberg, C Hu & K Carder, 2001. Change detection in shallow coral reef environments using Landsat 7 ETM+ data. Remote Sensing of Environment, 78: 150-162

36 Song C, C E Woodcock, K C Seto, M P Lenney & S A Macomber, 2001. Classification and Change Detection using Landsat TM Data. When and How to Correct Atmospheric Effects?. Remote Sensing of Environment, 75(2): 230-244

37. Spitzer D & R W J Dirks, 1987. Bottom influence on the reflectance of the sea. International Journal of Remote Sensing, 8(3): 279-290

38 Edwards A, 1999. Applications of Satellite and Airborne Image Data to Coastal Management. (Coastal region and small island papers 4, UNESCO)

39 Khan M A, Y H Fadlallah & K G Al-Hinai, 1992. Thematic mapping of subtidal coastal habitats in the western Arabian Gulf using Landsat TM data - Abu Ali Bay, Saudi Arabia. International Journal of Remote Sensing, 13(4): 605-614

40 Tassan S, 1996. Modified Lyzenga's method for macroalgae detection in water with non-uniform composition. International Journal of Remote Sensing, 17(8): 1601-1607

41 Jerlov N G, 1976. Marine Optics (Elsevier Oceanographic Series Volume 14, Elsevier Scientific Publishing Company)

42 Edwards F J, 1987. Climate and Oceanography. In: Key Environments: Red Sea, edited by A.J. Edwards & S.M. Head (Pergamon Press), 45-69

43 Kinsey D W, 1985. Metabolism, calcification and carbon production I: systems level studies. In: Fifth International Coral Reef Congress (EPHE, Tahiti), 505-526.

44 Houhoulis Smit P, 2001. Maximizing Information Content of Landsat Imagery for Coastal Zone pplications. Photogrammetric Engineering & Remote Sensing, 67(7): 769-771.

45 Huston M A, 1994. Biological diversity: the coexistence of species on changing landscapes (Cambridge University Press).

46 Landsat Project Science Office, last update: 29/04/2003, Landsat 7 Science Data Users Handbook, Chapter 11 – Data products, Accessed: 21/05/2003, http://ltpwww.gsfc.nasa.gov/IAS/handbook/handbook_htmls/chapter11/chapter11.html

47 Chavez P S Jr, 1996. Image-Based Atmospheric Corrections - Revisited and Improved. Photogrammetric Engineering & Remote Sensing, 62(9): 1025-1036

48 Gordon H R & A Morel, 1983. Remote Assessment of Ocean Color for Interpretation of Satellite Visible Imagery (Springer, New York)

49 Armstrong R A, 1993. Remote sensing of submerged vegetation canopies for biomass estimation. International Journal of Remote Sensing, 14: 621-627

50 Haydn R, G W Dalke & J Henkel, 1982, Application of the IHS color transform to the processing of multisensor data and image enhancement. In: Proceedings of the International symposium on remote sensing of arid and semi-arid lands (Cairo, Egypt), 599-616

51 Chavez P S Jr, S C Sides & J A Anderson, 1991. Comparison of Three Different Methods to Merge Multiresolution and Multispectral Data: Landsat TM and SPOT Panchromatic. Photogrammetric Engineering & Remote Sensing, 57(3): 295-303

52 Pohl C & J L Van Genderen, 1998. Multisensor image fusion in remote sensing: concepts, methods and applications. International Journal of Remote Sensing, 19(5): 823-854

53 Hochberg E J & M J Atkinson, 2000. Spectral discrimination of coral reef benthic communities. Coral Reefs, 19: 164-171

54 Zainal A J M, D H Dalby & I S Robinson, 1993. Monitoring Marine Ecological Changes on the East Coast of Bahrain with Landsat TM. Photogrammetric Engineering & Remote Sensing, 59(3): 415-421

55 Wagner T W, J L Michalek & R Laurin, 1991. Remote Sensing Applications in the Coastal Zone. In: Satellite Monitoring of Coastal Marine Ecosystems: A Case from the Dominican Republic, edited by R. Stoffle & D. Halmo (Consortium for International Earth Science Information Network, Michigan (USA)), p. 17-56

56 Michalek J L, T W Wagner, J J Luczkovich & R W Stoffle, 1993. Multispectral Change Vector Analysis for Monitoring Coastal Marine Environments. Photogrammetric Engineering & Remote Sensing, 59(3): 381-384

57 Luczkovich J J, T W Wagner, J L Michalek & R W Stoffle, 1993. Discrimination of Coral Reefs, Seagrass Meadows, and Sand Bottom Types from Space: A Dominican Republic Case Study. Photogrammetric Engineering & Remote Sensing, 59(3): 385-389

58 McManus J & M Noordeloos, 1998. Toward a Global Inventory of Coral Reefs (GICOR): Remote Sensing, International Cooperation, and Reefbase. In: Fifth International Conference on Remote Sensing of the Marine Environment (San Diego, USA), 83-89

59 Mumby P J, E P Green, A J Edwards & C D Clark, 1999. The cost-effectiveness of remote sensing for tropical coastal resources assessment and management. Journal of Environmental Management, 55(3): 157-166